3 Biotech (2023) 13:83
https://doi.org/10.1007/s13205-023-03496-0

ORIGINAL ARTICLE

Enriched adipose stem cell secretome as an effective therapeutic strategy for in vivo wound repair and angiogenesis

Amita Ajit[1] · T. Retnabai Santhosh Kumar[2] · V. S. Harikrishnan[3] · Arya Anil[3] · A. Sabareeswaran[4] · Lissy Kalliyana Krishnan[1]

Received: 18 June 2021 / Accepted: 24 January 2023 / Published online: 13 February 2023

Abstract

The therapeutic potential of adipose tissue-derived mesenchymal stem cells (ADMSCs) is well studied for use in non-healing wounds. However, concerns on the transplantable cell number requirement, cell expansion, cell viability, retained cell multipotency and the limited cell implantation time for efficient impact hinders cell therapy. Recent literature is much inclined to the superiority of the ADMSCs' secretome, pre-dominating its paracrine-mediated therapeutic impact. In this context, the possibility of attaining accelerated wound angiogenesis through non-viral mediated enrichment of the ADMSCs secretome with pro-angiogenic growth factors (AGF) seems promising. Accordingly, this study aimed to explore the effect of AGF-enriched ADMSCs secretome for accelerating wound angiogenesis and repair in acute large area full thickness excision rabbit wound model, as adopted from Salgado et al. (Chir Buchar Rom 108:706–710, 1990). Using sub-dermal single-dose injections along the margin of the dorsal wound, native ADMSCs secretome, AGF-enriched ADMSC secretome, allogenic rabbit ADMSCs and a combination of AGF-enriched ADMSC secretome with allogenic rabbit ADMSCs were transplanted independently. Twenty-eight days (28 days) post-transplantation, histopathological analysis was performed to assess the effect. Hematoxylin and eosin (H&E) staining showed enhanced epithelization, notable granulation tissue and collagen fiber deposition in AGF-enriched secretome transplanted groups. This was confirmed by elevated CD31 detection, faster wound closure time and collagen organization. The use of single-dose AGF-enriched ADMSCs' secretome for therapeutic angiogenesis and wound repair seems to be a promising cell-free therapeutic option. Further investigations using multiple doses on larger animal groups remains to be explored in order to ascertain the comparative potential of AGF-enriched ADMSCs' secretome.

Keywords Adipose stem cell secretome · Non-viral transfection · Enriched secretome · Angiogenesis · Full thickness wounds · Large area wounds · Rabbit model · Wound healing

✉ Amita Ajit
dr.amitaajit@gmail.com

T. Retnabai Santhosh Kumar
trsanthosh@rgcb.res.in

V. S. Harikrishnan
harikrishnan@sctimst.ac.in

Arya Anil
aryaanil.777@gmail.com

A. Sabareeswaran
asw@sctimst.ac.in

Lissy Kalliyana Krishnan
lissykrs@gmail.com

[1] Division of Thrombosis Research, Department of Applied Biology, Biomedical Technology Wing, Sree Chitra Tirunal Institute for Medical Sciences and Technology, Poojappura, Thiruvananthapuram, Kerala 695012, India

[2] Integrated Cancer Research, Rajiv Gandhi Centre for Biotechnology, Thiruvananthapuram, Kerala 695014, India

[3] Division of Laboratory Animal Science, Biomedical Technology Wing, Sree Chitra Tirunal Institute for Medical Sciences and Technology, Thiruvananthapuram, Kerala 695012, India

[4] Histopathology Laboratory, Department of Applied Biology, Biomedical Technology Wing, Sree Chitra Tirunal Institute for Medical Sciences and Technology, Thiruvananthapuram, Kerala 695012, India

Introduction

Numerous reports demonstrate that Mesenchymal Stem Cells (MSCs) either obtained from the same individual or from an allogenic stem cell donor, on administration, display curative potential in healing wounds and in regeneration of the skin tissue (Foubert et al. 2017). This is attained through their multi-potency, release of paracrine bio-factors, and cytokines (Foubert et al. 2017). Foubert et al. also highlight in their study that MSCs release cytokines that prevent tissue scarring and control the progression of hypertrophic scarring (Foubert et al. 2017). Lately, adipose-derived mesenchymal stem cells (ADMSCs) and ADMSCs secretome (also called the conditioned medium) seem significantly effective in enhancing hair growth, and in the advancement of functional sweat gland-like structures (Duscher et al. 2016). ADMSCs are also seen to promote both angiogenesis and vascular stability which is important for supply of nutrients for adequate regeneration and tissue repair (Jackson et al. 2007). Human adipose-derived mesenchymal stem cells (hADMSCs) are attractive candidates in tissue engineering with regard to their native copiousness, well standardized and easy tissue collection processes and their similarity to bone marrow stromal cells (BMSCs) in terms of differentiation potential (Tremolada et al. 2016). However, with due consideration to therapeutic angiogenesis in wound healing, composed growth in vasculature is crucial for successful regeneration. There is noticeable indication supporting MSCs' major contribution through paracrine backing of angiogenesis. Outstandingly, MSCs may harbor an altered angiogenic potential based on their tissue of origin. Reports state that ADMSC secretome presents a better tubulogenic competence compared to BM-MSCs due to their higher expression of angiogenic factors (Maacha et al. 2020). Though numerous studies in animal disease models report efficacy, ADMSCs' therapy even now faces constraints due to the inadequacy of these cells to secrete sufficient paracrine factors (Keeney et al. 2013). In this context, recent research has focussed on developing various approaches that could modify the ADMSCs secretome profile in such a way that it can adequately deliver the desired therapeutic efficacy (Ranganath et al. 2012). The transfer of angiogenic genes via non-viral vectors in ADMSCs, to momentarily deliver the growth factors in order to drive adequate angiogenesis offers promise (Laiva et al. 2018). Previous work has shown that, along with the transfection mediated increase in release of VEGF, and the stem cell secreted factors, it is possible to attain greater angiogenesis, reduced cell apoptosis, and improved tissue survival, relative to the use of VEGF protein alone. Also, latest reports reveal that supply of several pro-angiogenic GFs either in as in a cocktail form or consecutively, can trigger speedy neovascularization throughout wound healing (Park and Gerecht 2014). In this study, we explored in vivo application of hADMSCs secretome upon transient non-viral mediated over-expression (lasting 14 days) of two well-known angiogenic mediators i.e. VEGF-A and HIF-1α, using previously established protocol (Ajit et al. 2019a). Considering cell therapy to be decidedly managed by global authorities to guarantee biosafety and efficacy and that it is noteworthy to identify that MSCs from diverse sources might have dissimilar immunomodulation proficiencies with different capacities to multiply and differentiate (Hu et al. 2010), the current study also focused to investigate in vivo efficacy of engineered secretome over allogenic cell transplantation.

Methods

Generation of engineered hADMSCs' secretome

Adipose tissue lipoaspirates were collected from 6 donors of both genders, within the age group of 25–45 undergoing cosmetic surgery. hADMSCs were isolated and cultured till Passage 3 (Ajit et al. 2019b).. Engineered hADMSCs over-expressing angiogenic growth factors was then generated, as described previously (Ajit et al. 2019b). Briefly, 5×10^6 cells/mL of hADMSCs were transfected using Neon® Transfection System (Cat No: MPK1096, Invitrogen). The mammalian plasmids encoding human VEGF-A (Cat No: HG11066-ACG, Sino Biological Inc, China) and Hif-1α (Cat No: HG11977-ACG, Sino Biological Inc, China) were also used. Secretome of engineered h-ADMSCs (s-e-hADMSCs), was obtained by pooling the supernatant of transfected and cultured cells on day 2, 4, 6, 8, 10, 12 and 14, followed by centrifugation at 400*g* (1500 rpm), for 6 min and was quantitatively assessed for over expressed angiogenic factors (AFs) by ELISA as reported previously (Ajit et al. 2019b).

Isolation of allogenic rabbit ADMSCs and cell labelling

Adipose tissue from rabbits (~ 10 g) was surgically collected and ADMSCs were isolated and expanded in culture by standard protocol. Passage 3 rabbit ADMSCs (rADMSCs) were then tagged using General PKH26 -GL cell linker kit (Sigma®), a fluorescent vital dye as instructed by the manufacturer.

Creation of large excision acute wounds

Generation of in vivo wounds was performed on in-bred New Zealand White Male Rabbits ($n = 21$, aged (9–12 months);

weighing between 2500 and 2800 g). Experimental animals were contained in separate cages and were provided food and water, ad libitum. The care and management of animals were as per ISO 10993—Part-II and CPCSEA guidelines. For the study, the animals were anesthetized using 50 mg/kg of ketamine hydrochloride and 5 mg/kg of xylazine (I/M). The excision wounds were made on the dorsal skin of the rabbits which were symmetrically positioned in sternal recumbence. At 10 cm from the iliac crest and 14 cm from the cranial border from the 7th cervical vertebra set the caudal border for the field of operation. Residual hairs were also removed with commercial depilatory crème. Two acute, square (4 × 4 cm^2) full thickness excision skin wounds were created per animal for understanding wound healing in large wounds (Salgado et al. 2013) as shown in Fig. 1.

Transplantation studies

Among the created full thickness wounds, control sites were treated with standard betadiene ointment. Treatment sites constituted of seven different treatment strategies including allogenic rADMSCs with or without the transfected hADMSC secretome or with the transfected hADMSCs secretome or the secretome alone as shown in Table 1. The test samples were introduced at four sites alongside the margins of the wound through sub-dermal injections (Pelizzo et al. 2015). Each wound group received either 1.0×10^6 rADMSCs cells or transfected hADMSC's secretome containing ~ 1400 pg of VEGF or Hif-1α, independently or in combination (1:1). After transplantation, the wound was covered by non-irritant transparent bio-occlusive dressing. Every two days, the dressing was replaced with a fresh one to uphold a wet wound environment. Rabbits did not receive any immune suppression. Rabbits were injected with 10 mg/kg of ampicillin cloxacillin (10 mg/kg) two times daily and 0.6 mg/Kg of Meloxicam once daily. The wounds were observed daily and snapped using a digital camera.

Table 1 List of wound healing groups for transplantation study

Group I	Sham wounds (untreated control)
Group II	Treated with VEGF-s–e-hADMSCs
Group III	Treated with HIF-1α–s–e-hADMSCs
Group IV	Treated with s–n-hADMSCs
Group V	Treated with rADMSCs and VEGF-s–e-hADMSCs
Group VI	Treated with rADMSCs and HIF-1α–s–e-hADMSCs
Group VII	Treated with rADMSCs

VEGF over expressed secretome of engineered hADMSCs (VEGF-s–e-hADMSC); HIF-1α over expressed secretome of engineered hADMSCs (HIF-1α–s–e-hADMSCs); Secretome of non-engineered hADMSCs (s–n-hADMSCs); Rabbit ADMSCs (rADMSCs)

Post 28 days, the animals were sacrificed, their wound sites were harvested and the tissue was processed for evaluation of wound healing.

Bio-distribution of rADMSCs following sub-dermal administration

Explanted wound skin samples from groups (test and control) that received labelled rADMSCs were assessed for retainment of transplanted cells within the site of transplantation using IVIS Spectrum in vivo Imaging System (PerkinElmer, USA). Tissues were fluorescently imaged (745/800 em/ex filters) through epi-fluorescence. The captured mages were then examined using Living Image 4.3.1 software. The regions of interest (ROI) were manually defined and an average radiant efficiency was premeditated after deducting the noise signal (Luli et al. 2016).

Histological analysis

The harvested wound site tissues were fixed in 10% neutral-buffered formalin. The fixed tissues were then entrenched in paraffin blocks from which sections of 5 µm thickness

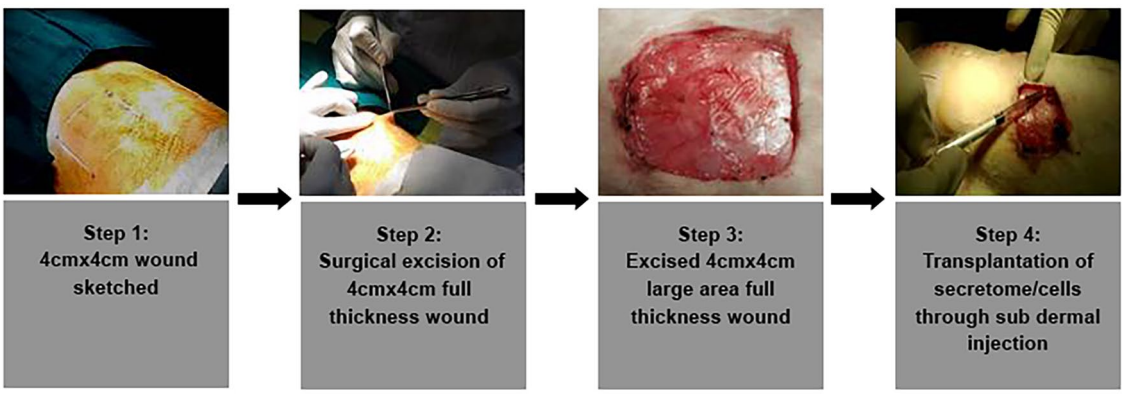

Fig. 1 Step wise illustration of the excision full thickness rabbit wound and transplantation route

subjected to staining with hematoxylin and eosin (H&E), Direct Red 80 for collagen fibers, and CD31 for detection of neo-vascularization.

Hematoxylin and eosin staining

Tissue sections were H&E stained to correlate the rate of tissue re-epithelization rate and overall infiltration of inflammatory cells. The fixed tissue specimens were handled regularly in an automatic tissue processor (ASP300, Leica, Germany) and then entrenched in paraffin. Using a rotary microtome (RM2550, Leica, Germany), 5-micron thin sections were sliced and then stained with H&E. Histopathologic examinations were assessed by light microscope (Nikon E 600, Nikon, Japan) and photomicrographs were photographed using the microscope attached camera (Nikon DsR1, Nikon, Japan). A single pathologist at the Institute, blinded to all information regarding the groups performed the gross and histopathologic examination of the tissues.

Immunohistochemistry

Signs of vascularization within the newly developed tissue is often regarded as the hallmark of healing. A noteworthy rise in the density of blood vessels is detected in during the proliferative phase of healing as compared to what is seen in an uninjured skin (Johnson and Wilgus 2014). To determine effect of transplantation in accelerated neo-vascularization, an endothelial specific marker CD31, was assessed in each group by immunohistochemical analysis**.** As per the protocol described earlier (Pelizzo et al. 2015) deparaffinized tissue sections were hydrated and treated with 10 mM citrate buffer for antigen retrieval. Tissues were then treated with 3% hydrogen peroxide for 15 min to quench the endogenous peroxidases. Tissues were then incubated with Fetal Bovine Serum to block all nonspecific antibody binding. Immunohistochemistry using anti-human CD31/PECAM1 antibody (Biolegend), which cross-reacts with rabbit endothelial cells recognized the endothelial cells within the tissue. Briefly, overnight incubation of the sections at 4 °C with 1:500 anti-human CD31 antibody or bovine serum albumin (which served as a negative control) was done, there after the sections were subjected to horseradish peroxidase conjugated anti-rabbit immunoglobulin (Abcam) for 2 h at RT. This was then subjected to 5 min incubation with 3,3′-diaminobenzidine (DAB; Sigma). Lastly, the mounted sections were inspected using a light microscope. ImageJ software was used for image analysis. Using freehand selection tool, neoplastic granulation area was defined. Using colour deconvolution plugin DAB-stained areas were distinguished. A threshold was set to analyze the brown images using bins. The percentage of the positive area was measured with the Analyze Particles function (Ruifrok and Johnston 2001).

Direct red 80 staining

To assess the degree of collagen synthesis and organization, Direct Red-80 (Sigma) (also called pico-Sirus red stain) was used (Fujita et al. 2017). Briefly, de-waxed and hydrated paraffin sections were nuclei stained with Weigert's haematoxylin for 8 min and washed for 10 min in running tap water. The picro-sirius red stain was then added and incubated for 1 h which gives near-equilibrium staining. The sections were then washed with two changes of acidified water, dehydrated in three changes of 100% ethanol, cleared in xylene and mounted in a resinous medium. Bright-field images were captured. The fiber density of neoplastic granulation under the wounds was analyzed on images of random areas captured using a 20× lens. The percentages of colored area in the images were quantitatively assessed with ImageJ.

Semi-quantitative analysis of histological parameters

The presence of differentiated multi-layered epithelium, inflammatory cells, and the collagen content in granulation tissue of dermis were observed microscopically as explained above and assessed using a semi-quantitative scale, with scores ranging from 1 to 4 as reported in Table 2. Healing status was graded as good (19–24), fair (12–18) and poor (8–11) as adopted (Gupta and Kumar 2015) and modified (Table 3).

Statistical analysis

All experiments were independently performed in triplicates using with three different donor cells. Statistical evaluations were made using one-way analysis of variance (ANOVA) or student's *t* test, as appropriate. Post-hoc Bonferroni correction was used for multiple comparisons. Standard deviations (SD) and mean values were derived for all parameters and denoted in graphical form. Significance is depicted as ***($P < 0.001$); **($P < 0.01$); and *($P < 0.05$). In each figure

Table 2 Parameters assessed to calculate healing score

Score	4	3	2	1
Amount of granulation tissue	Profound	Moderate	Scanty	Absent
Inflammatory infiltrate	Negligible	A Few	Moderate	Plenty
Collagen fiber orientation	Vertical	Mixed	Horizontal	–
Pattern of collagen	Reticular	Mixed	Fascicle	–
Amount of early collagen	Profound	Moderate	Minimal	Absent
Amount of mature collagen	Profound	Moderate	Minimal	–

Table 3 Healing scores analysis

Groups	Amount of granulation tissue	Inflammatory infiltrate	Collagen fiber orientation	Pattern of collagen	Amount of early collagen	Amount of mature collagen	Total score
Sham (control)	2	4	3	2	2	2	**15**
Vegf-s–e-hADMSCs	4	4	4	4	3	3	**22**
Hif-1α-s–e-hADMSCs	4	4	3	4	2	4	**21**
Vegf-s–e-hADMSCs + rADMSCs	4	4	4	4	4	3	**23**
Hif-1α-s–e-hADMSCs + rADMSCs	4	4	3	4	3	3	**21**
s–n-ADMSCs	3	4	3	2	2	4	**18**
rADMSCs	3	4	3	2	2	2	**16**

Using this healing score, it is concluded that test groups in the study were correlated with accelerated wound healing in comparison to the sham group ($n = 3$)

legend, details on number of replicate experiments executed is specified.

Results

Characteristics of rabbit ADMSCs

Combinatorial effect of hADMSC over-expressed secretome was used in the presence of transplanted rabbit ADMSC. Spindle shape morphology and adherence to plastic was shown by rabbit ADMSCs (rADMSCs) that were isolated and cultured from multiple allogenic donor tissues (Fig. 2A). Before transplantation rADMSCs were tagged with PKH26 to track transplanted cells in the host upon termination. Imaging detected red fluorescence emitted by PKH26 bound to the rADMSCs cell membrane as seen in (Fig. 2B).

Ex vivo identification of transplanted rADMSCs by using IVIS®

Fluorescence detection determined that transplanted rADMSCs migrated to distant sites: but, when transplanted along with the s-e-hADMSCs, the cells were retained for 28 days near to the injury at the site of injections as evidenced in Fig. 3. We assume that this observation could possibly relate to the paracrine effects of the enriched secretome that extend the residence time in. The wound area for localization and retainment of the transplanted stem cells that could also give way to improving the effectiveness of cellular therapies. However, a comparison with non-engineered secretome is required to validate if this effect pertains only to the enriched secretome itself or the given stem cell secretome as such**.** Cell density in the tissue is represented by a color bar scale where red indicates a relative high cell density while blue indicates a relative low cell density.

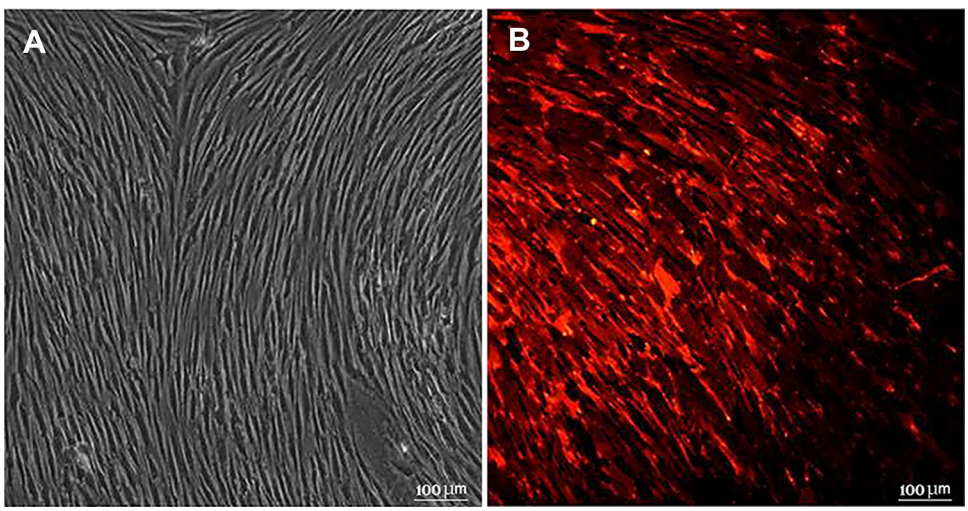

Fig. 2 Isolation and culture of rADMSCs. **A** Micrograph of isolated and cultured rADMSCs showing typical spindle shape morphology (20×) **B** rADMSCs labelled with PKH26 as observed by fluorescence microscopy (20×)

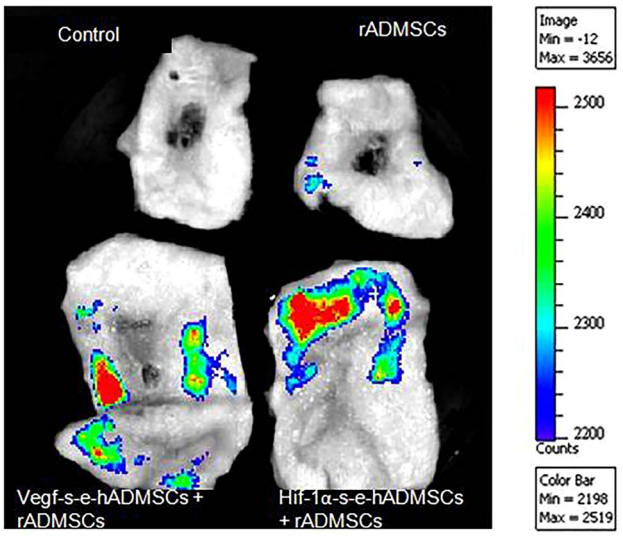

Fig. 3 Transplanted cells tracked using fluorochrome images. Representative images of skin explants from control and experimental groups analyzed with IVIS® for the presence of PKH26 labeled cells obtained by manual alignment of the spectrum. The color scale bar shows the range of strongest to weakest signal. The intensity is strongest for the red color points. The darker the spot, the stronger the signal

Visual observation of surface wound healing in rabbits

The photographs of postoperative wound healing in control (sham) and treatment groups for 5, 10, 15 and 28 days, with respect to each individual and respective wound site is shown in Fig. 4A. The large wound areas attained significantly better closure when treated with s-e-hADMSCs in comparison to the sham-control group. 47% of wound closure was achieved on 10d in wounds treated with Vegf-s-e-hADMSCs vs. 19% for control-sham wounds as computed and quantified (Fig. 4B).

Microscopic observations of H&E-stained sections

Histological analysis of the wounds of all respective groups of treatment and control were performed by H&E staining. The healing rate of groups treated independently with s-e-hADMSCS (Fig. 5) was notably high in contrast to groups treated independently with s–n-hADMSCs and rADMSCs (Fig. 6A) and to groups treated in combination of both s–e-hADMSCs with rADMSCs (Fig. 6B). 28 days post generation of the wound, epithelialization and angiogenesis was apparent in tissue samples treated with s–e-hADMSCS, independently and in combination with rADMSCs groups. Mature granulation tissues were seen. Low number of fibroblasts were seen whereas collagen fiber deposition was evidenced. Very few inflammatory cells were seen in the wound area.

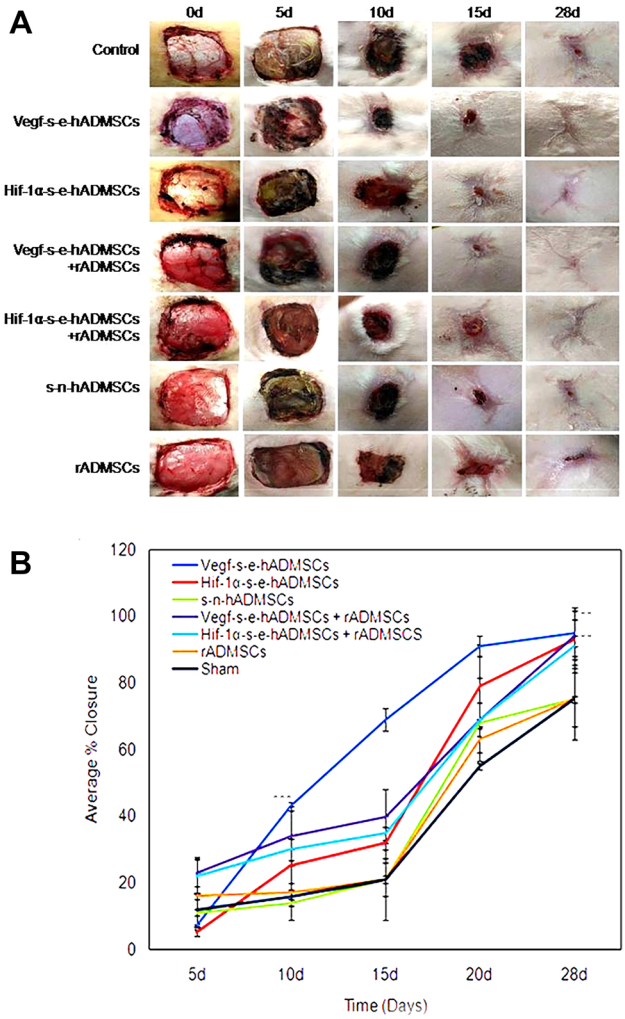

Fig. 4 **A** Representative images demonstrating progression of Wound Closure: seven different full thickness excision wound groups in the study of the same dimension (4 cm × 4 cm) were gross imaged on 0 day, 5 days, 10 days, 15 days and upon termination on 28 days. Comparative analysis showed potential of Vegf-s-e-hADMSCs to accelerate the rate of excision wound closure in vivo by 10d. Complete wound closure was observed in s–e-hADMSCs groups, both independently and in combination with rADMSCs at 28 days, ($n=3$). **B** Graphical representation of wounds closure: The wound area measured during the animal evaluation at 0 days, 5 days, 10 days, 15 days and upon termination on 28 days was computed and analyzed. Wound closure demonstrates the effect of seven different types of application highlighting potential of s–e-hADMSCs, both independently and in combination with rADMSCs. Error bars represent standard deviation, ***($P<0.001$); **($P<0.01$); and *($P<0.05$) vs non electroporated hADMSCs, $n=3$

Microscopic analysis of collagen-stained sections

Specific staining of the extracellular matrix (ECM) components such as collagen is helpful in studying tissue

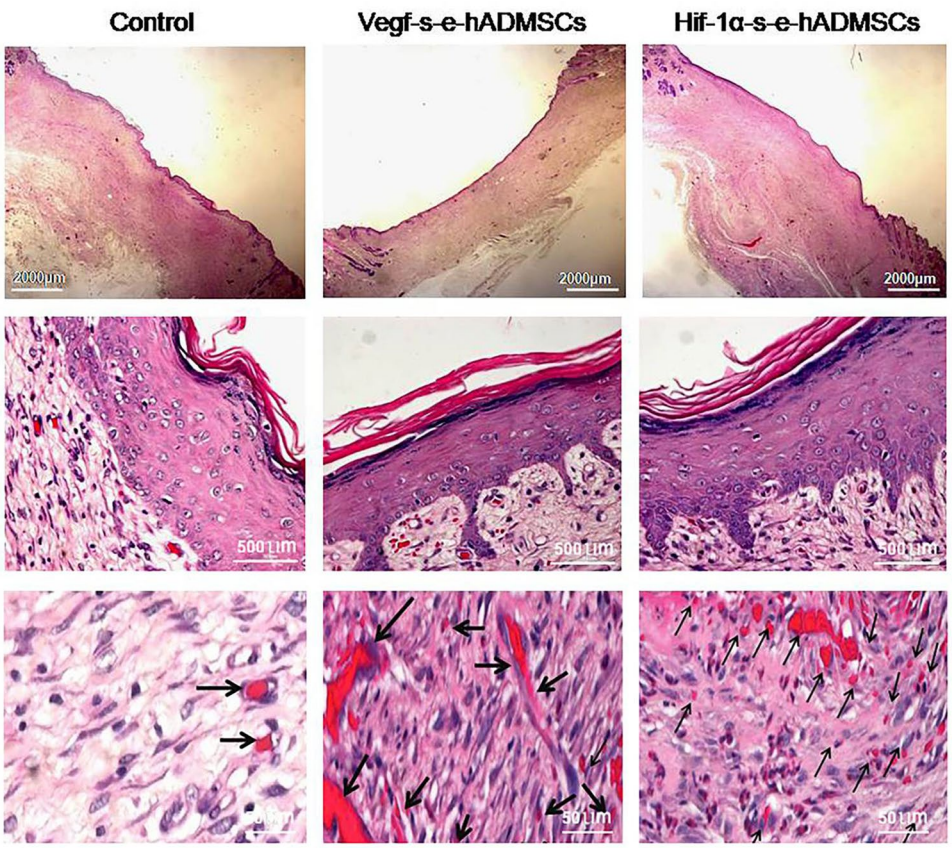

Fig. 5 Representative images of H&E stained tissue sections. Photomicrograph of histopathological section of wound tissue 28 day after creation of wound (H&E) in large area full thickness rabbit wound groups without treatment (Control) and with treatment (Vegf-s–e-hADMSCs and Hif-1α-s–e-hADMSCs). As evident in figures, no-treatment samples showed incomplete epidermis, poor vascularization and no rete pegs at the same time. Treated groups have well organized epidermis with developed rete pegs and neo-vascularized dermis layers (black arrows) at day 28 of treatment. Top panel images at Scale bar = 2000 µm, middle panel images at scale bar = 500 µm, bottom panel images at scale bar = 50 µm, respectively, ($n = 3$)

remodelling. In this study, Sirius red stain which selectively highlights collagen network detected the presence of mature collagen. Fibres that turned bright red depicted presence of thick, high-density collagen in groups treated with the secretome alone and in the combination groups (secretome + rADMSCs) as compared to the control groups treated with saline, where the staining shows presence of disorganized collagen fibres Fig. 7A. With the help of ImageJ software, the areas detected by Sirius red stain showing the presence of mature collagen were measured and represented in terms of percentage. On comparison of the results obtained from each study group, it was observed that wounds treated with the secretome had the presence of a significantly larger area of mature collagen than those in the control groups Fig. 7B.

Effect of treatment on vascularization of regenerated skin

Presence of endothelial marker CD31 was investigated in the tissue sections to confirm new capillary vessels formed within the granulation tissue. In groups treated with s-e-hADMSCs and in combination (s–e-hADMSCs + rADMSCs), wide capillary network with broader vessels were detected as compared with groups that received saline alone Fig. 8A. Significant number of capillaries were also detected in groups treated with s-e-hADMSCs as compared to the control as seen in Fig. 8B.

Semi-quantitative analysis of histological parameters

The regenerated epithelial layer features, inflammatory infiltrate extent and collagen deposition in wound groups were as assessed semi-quantitatively post 28 days and is reported in Table 1. In the current investigation, the best and worst re-epithelization rates were considered after transplantation. The healing score analysis establishes healing status graded as good for groups treated with s-e-hADMSCs, both independently and in combination with rADMSCs; whereas, all other groups were graded fair.

Discussion

In the context of wound healing research, the generation of preclinical or in vivo wound healing models that exhibit comparable or similar characteristics of healing to what is seen clinically is a challenge (Andrade et al. 2017). In vivo mouse and rat models find restricted use in skin research

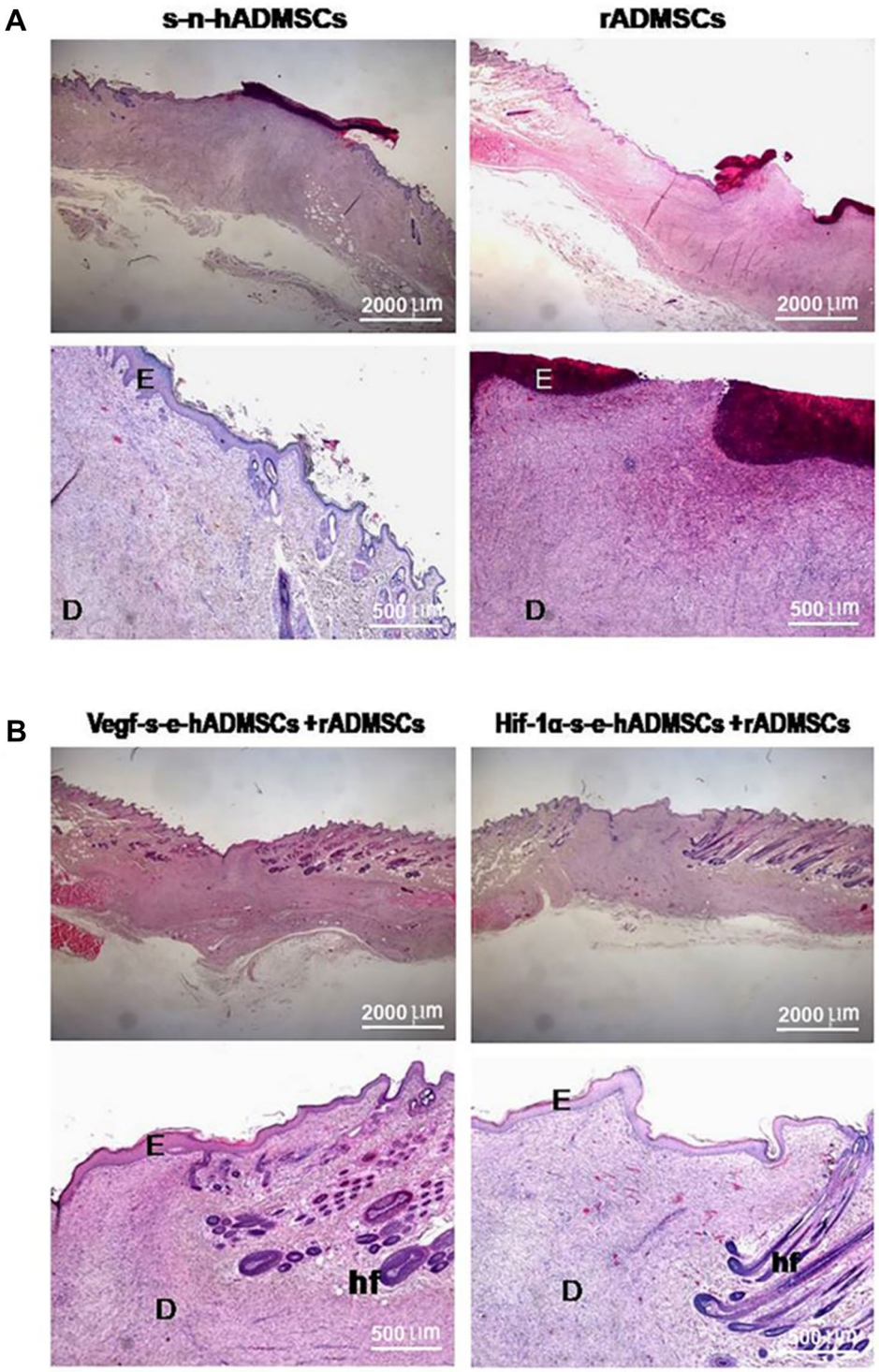

Fig. 6 Representative images of H&E stained tissue sections: Photomicrograph of histopathological section of wound tissue 28 day after creation of wound (H&E) in large area full thickness rabbit wound groups with treated with s–n-hADMSCs, rADMSCs, (Vegf-s–e-hADMSCs + rADMSCs) and (Hif-1α-s–e-hADMSCs + rADMSCs), respectively. As evident in figures, s–n-hADMSCs and rADMSCs groups display poor epithelisation and incomplete healing. Groups treated with (Vegf-s–e-hADMSCs + rADMSCs) and (Hif-1α-s–e-hADMSCs + rADMSCs) display complete epithelisation and healing. Letter 'E' depicts epidermis, Letter 'D' depicts dermis and 'hf' depicts hair follicles. Scale bar (= 500 µm & 2000 µm), ($n = 3$)

owing to significant histological and physiological differences in the layers of their skin as compared to that of human skin (Wong et al. 2011; Dorsett-Martin 2004). On the other hand, in vivo pig models, have closer similarities to that of human skin but their use in experimental research is hindered due to their increased cost of animal maintenance and husbandry. Researchers have hence pioneered the rabbit model for wound healing research with due consideration to their affordability, sufficient size for generation of larger wounds and their close histopathological similarities to human skin (Billingham and Medawar 1951; Grada et al. 2018). Accordingly, the rabbit model was chosen in this study for generation of large area full thickness excision wounds. In the generated wounds, we assessed the

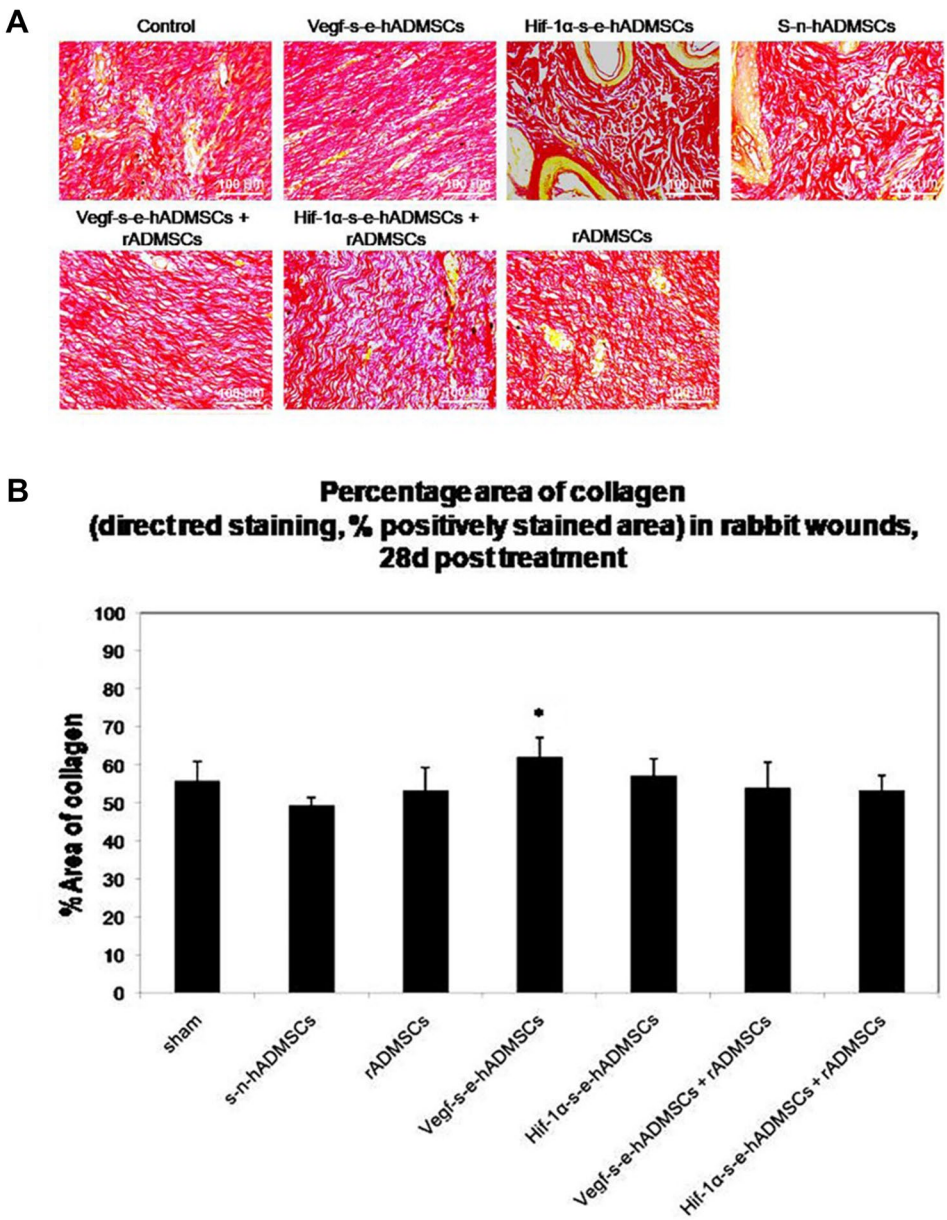

Fig. 7 Representative images demonstrating collagen deposition. **A** Sirius Red stained sections depicting collagen deposition and organization in control and treated groups. Scale bar = 100 µm, ($n = 3$). **B** Comparison of percentage area of collagen: Sirius Red staining, Percentage area occupied by positively stained collagen fibers in relation to the total repair area in rabbit wounds, 28 days post treatments. Vegf-s–e-hADMSCs and Hif-1α-s–e-hADMSCs show significant effect in deposition of collagen [$n = 3$, Error bars represent standard deviation, ***($P < 0.001$); **($P < 0.01$); and *($P < 0.05$) vs sham (control)]

angiogenic efficiency of s–e-hADMSCs, both independently and in combination with allogenic rabbit ADMSCs. The results showed migration of ADMSCs from their site of transplantation to distant regions establishing their transmigration potential as reported earlier (De Becker and Riet 2016). We also observed an enhanced homing of the transplanted rADMSCs when administered in combination with s-e-hADMSCs as compared to the independent administration of rADMSCs. This shows that the cytokines within the s-e-hADMSCs did favour the stem cell homing. Our finding does correlate to similar studies that report enhanced BMSC homing upon transplantation, with an increase in cytokine expression (Ziadloo et al. 2012). Further, on gross observation of wound closure, it was seen that the wounds treated with s-e-hADMSCs achieved better closure compared to the wounds in the control group. On the 10th day, 47% of wound closure was achieved in wounds treated with Vegf-s–e-hADMSCs compared to the 19% of closure seen in the control wounds. Though a complete closure was not obtained at the 10th day, the result does promise a lesser exposure area of the connective tissue for a faster wound healing. Also, a lesser risk for contamination is indicated as evidenced by their higher average percentage closure patterns on 15th, 20th and 28th days (Fig. 4B). We further assessed the different wound groups through histological assessment using H&E staining. This ensured that there was no apparent inflammatory response such as infection, fistula, or fibrous capsule detected at either the implanted sites or its

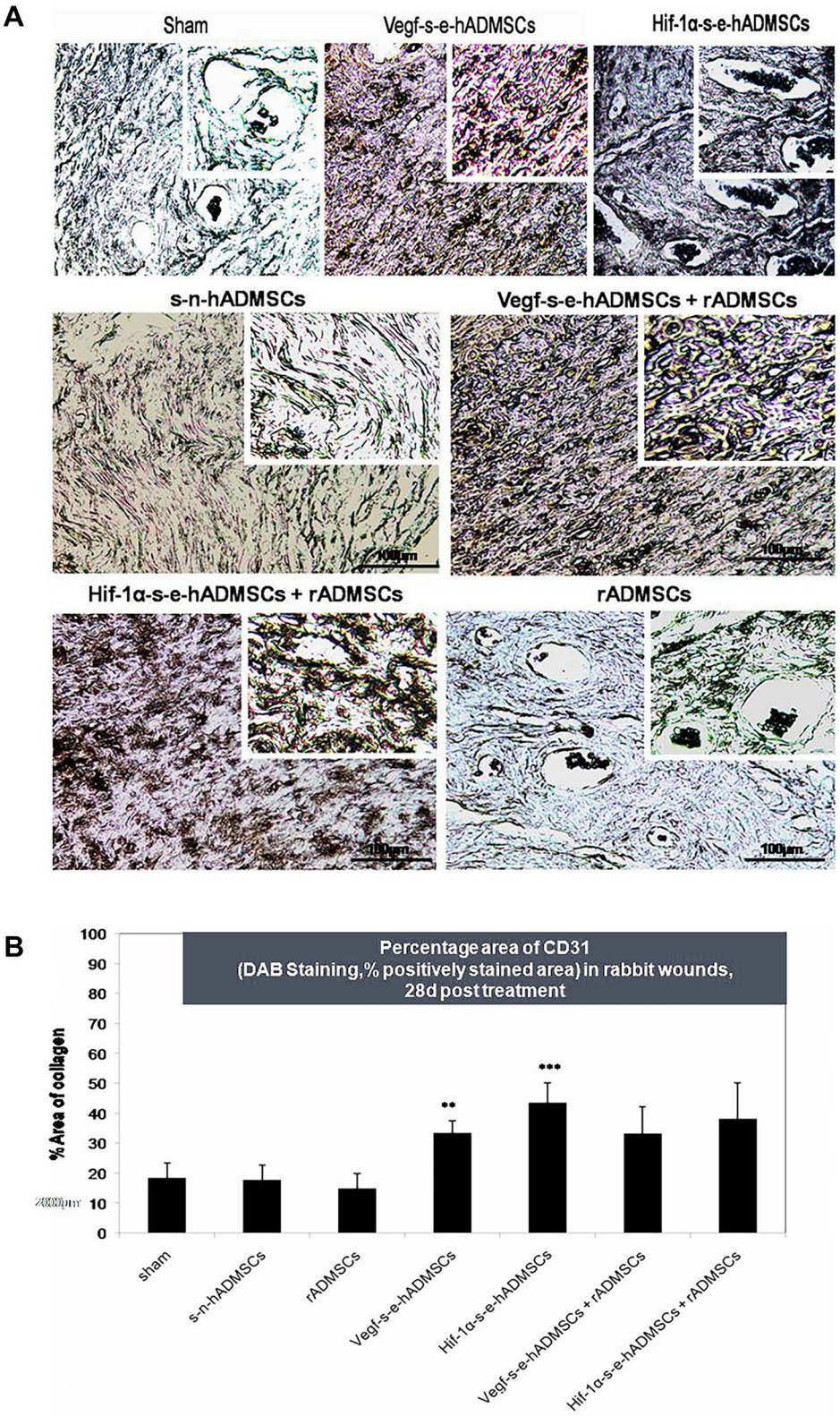

Fig. 8 Blood vessel staining in rabbit skin wounds. **A** CD-31 (PECAM-1) is expressed by endothelial cells and CD-31 immunostaining is commonly used to identify blood vessels (indicated by brown staining). Representative images are shown of the centre of the excision wounds after 28 days of healing. Scale bar = 100 µm, $n = 3$. Insert scale bar = 50 µm **B** Percentage area of CD31 (DAB Staining, % positively stained area) in rabbit wounds, 28d post treatment. Vegf-s–e-hADMSCs and Hif-1α-s–e-hADMSCs show significant angiogenic potential in terms of CD31 expression in comparison with sham (control), ($n = 3$). Error bars represent standard deviation, ***($P < 0.001$); **($P < 0.01$); and *($P < 0.05$) vs. sham (control)

adjacent sites in all groups, post-transplantation. The results also indicated a noteworthy enhancement of wound healing in groups treated with s–e-hADMSCS both independently and in combination with rADMSCs as compared to other groups. The results confirmed the presence of reconstructed epidermis or epithelialization and evident angiogenesis. We

also observed a significantly larger presence of mature collagen in groups treated with the secretome as compared to the control groups. Moreover, endothelial specific, CD31 detection also showed additional widely distributed capillary network having broader vessels in those wounds that were independently treated with s–e-hADMSCs and in combination with rADMSCs when compared to their control wounds. We further keenly observed the s–e-hADMSCs treated wound groups, which showed a noteworthy presence of a well-organized epidermis with developed rete pegs and neo-vascularized dermis layers at 28 days of treatment in comparison to the other groups. Despite use of only a single-dose application of s–e-hADMSCs at day 0 for this study, it was interesting to observe the presence of elevated granulation tissue deposition at 28 days. This observation suggests that tissue repair stimulated by exogenous GFs persisted. This finding also falls in line with an earlier report on single-dose topical VEGF application in wound healing (Galiano et al. 2004). The outcome of this study thus gives an insight to the enhanced benefit of using s–e-hADMSCs alone. Even though survival and localization of transplanted rADMSCs was enhanced when administered in combination with s–e-hADMSCs in comparison to independent administration of rADMSCs, the overall effect of using s–e-hADMSCs alone stood much superior in wound healing. Additionally, combination of rADMSCs with s–e-hADMSCs did not improve angiogenesis or healing significantly as compared to the effect of s–e-hADMSCs alone. Literature does support that it is the secretome of hADMSCs that augment angiogenesis through paracrine activity and guided endothelial trans-differentiation rather than the direct replacement-mediated participation of the transplanted cell (Mitchell et al. 2019). Literature has also established capacity of MSCs-derived cell-free secretome to bring about several properties/effects as defined for the MSCs themselves. Pro-regenerative properties of MSCs secretome to modulate the immune system, to prevent cell death and fibrosis, to arouse vascularization, to encourage tissue remodelling, and to take on other cells is already well known (Ferreira et al. 2018; Choudhry and Harris 2018; Ajit and Ambika Gopalankutty 2021), which further substantiates our finding. At an in vivo perspective, it is thus concluded through this study that administration of engineered hADMSCs secretome alone promises a cell-free therapy for wound healing. Moreover, the achieved effective angiogenesis and wound healing of large area acute full thickness wounds using only a single dose or onetime application of the engineered secretome is the major highlight of this study. On considering the quantity and multiple dose requirement of recombinant VEGF at clinical practice which is quiet unaffordable, the use of a single-dose engineered hADMSCs secretome strategy could pave way to produce a cost effective treatment option. Surprisingly, we see that only few researchers have explored angiogenic effect of preconditioned MSCs's secretome profile in cutaneous healing. Our findings seem encouraging for wound healing researchers to (i) further explore the long-term effects of engineered secretome for establishing efficacy at translation, (ii) to explore the proteins and exosome composition of the bioengineered secretome, for therapeutic use facilitating a cellfree therapy, (iii) to explore the requirement of multiple applications for healing of chronic wounds (iv) to conduct further studies that are needed to rule out possible adverse effects for effective translation, (v) to look into scar and hair follicle growth in a long duration study and (vi) to finally study secretome under all three situations; VEGF, HIF-1alpha and their combination which stands significant in terms of choice of application, be it independently or in combination, with regard to wound size, wound type and the patient age.

Conclusion

Our preclinical in vivo study demonstrated angiogenic potential on applying the secretome comprising angiogenic growth factors (AGF) released into the medium upon engineered hADMSCs' culture. The application of such over-expressed and released AGFs elevated CD31 in 28 days of the experiment. Neither the secretome of non-engineered hADMSCs nor the transplantation of rADMSCs showed comparable expression of the angiogenic marker. As the secretome from engineered hADMSCs is a mixture of different growth factors; this preliminary study has not identified the exact molecule responsible for this increased angiogenesis. It could be a combinatorial or synergistic effect of different molecules. The highlight of this study is that the engineering of adipose-derived human stem cells facilitates the safe use of cell-free angiogenic growth factor application for accelerating wound regeneration resulting in ECM deposition and angiogenesis. Also, a single dose of s-e-hADMSCs producing therapeutic angiogenesis and wound regeneration is a much realistic option for clinical translation. This proven technology of non-viral human stem cell engineering and demonstration of in vivo wound regeneration and angiogenesis opens up room for effective investigations on profiling the s-e-hADMSCs. This would help identify the effective molecules and delineate the mechanism of action. Multiple dose experimentations on larger animal models could ascertain the application of this safe technology for clinical translation.

Acknowledgements The Director, SCTIMST and the Head, BMT Wing is duly acknowledged for extending the necessary facilities to implement this study. The technical support provided by Mr. Prakash R P and Mr. Shankar, Integrated Cancer Research-RGCB to perform electroporation is highly valued. The authors thank Ar. Jobin Joseph Abraham for the technical help in Manuscript Image formatting.

Funding The study was supported by the Women Scientist Scheme-A (WoS-A) grant awarded to Dr. Amita Ajit, which is funded by the Department of Science and Technology, Government of India.

Data availability statement All data associated with this study is provided in the manuscript.

Declarations

Conflict of interest The authors declare no competing interests.

References

Ajit A, Santhosh Kumar TR, Krishnan LK (2019a) Engineered human adipose-derived stem cells inducing endothelial lineage and angiogenic response. Tissue Eng Part C Methods 25:148–159. https://doi.org/10.1089/ten.tec.2018.0333

Ajit A, Santhosh Kumar TR, Krishnan LK (2019b) Engineered human adipose-derived stem cells inducing endothelial lineage and angiogenic response. Tissue Eng Part C Methods 25:148–159. https://doi.org/10.1089/ten.TEC.2018.0333

Ajit A, Ambika Gopalankutty I (2021) Adipose-derived stem cell secretome as a cell-free product for cutaneous wound healing. 3 Biotech 11:413. https://doi.org/10.1007/s13205-021-02958-7

Billingham R, Medawar P (1951) The technique of free skin grafting in mammals. J Exp Biol 28:385

Choudhry H, Harris AL (2018) Advances in hypoxia-inducible factor biology. Cell Metab 27(2):281–298

de Andrade ALM, Parisi JR, Brassolatti P, Parizotto NA (2017) Alternative animal model for studies of total skin thickness burns. Acta Cir Bras 32:836–842. https://doi.org/10.1590/s0102-86502017010000000005

De Becker A, Riet IV (2016) Homing and migration of mesenchymal stromal cells: how to improve the efficacy of cell therapy? World J Stem Cells 8:73–87. https://doi.org/10.4252/wjsc.v8.i3.73

Dorsett-Martin WA (2004) Rat models of skin wound healing: a review. Wound Repair Regen off Publ Wound Heal Soc Eur Tissue Repair Soc 12:591–599. https://doi.org/10.1111/j.1067-1927.2004.12601.x

Duscher D, Barrera J, Wong VW et al (2016) Stem cells in wound healing: the future of regenerative medicine? A mini-review. Gerontology 62:216–225. https://doi.org/10.1159/000381877

Ferreira JR, Teixeira GQ, Santos SG et al (2018) Mesenchymal stromal cell secretome: influencing therapeutic potential by cellular pre-conditioning. Front Immunol. https://doi.org/10.3389/fimmu.2018.02837

Foubert P, Zafra D, Liu M et al (2017) Autologous adipose-derived regenerative cell therapy modulates development of hypertrophic scarring in a red Duroc porcine model. Stem Cell Res Ther 8:261. https://doi.org/10.1186/s13287-017-0704-1

Fujita K, Nishimoto S, Fujiwara T et al (2017) A new rabbit model of impaired wound healing in an X-ray-irradiated field. PLoS ONE 12:e0184534. https://doi.org/10.1371/journal.pone.0184534

Galiano RD, Tepper OM, Pelo CR et al (2004) Topical vascular endothelial growth factor accelerates diabetic wound healing through increased angiogenesis and by mobilizing and recruiting bone marrow-derived cells. Am J Pathol 164:1935–1947. https://doi.org/10.1016/S0002-9440(10)63754-6

Grada A, Mervis J, Falanga V (2018) Research techniques made simple: animal models of wound healing. J Invest Dermatol 138:2095-2105.e1. https://doi.org/10.1016/j.jid.2018.08.005

Gupta A, Kumar P (2015) Assessment of the histological state of the healing wound. Plast Aesthetic Res 2:239. https://doi.org/10.4103/2347-9264.158862

Hu Y-L, Fu Y-H, Tabata Y, Gao J-Q (2010) Mesenchymal stem cells: a promising targeted-delivery vehicle in cancer gene therapy. J Controlled Release 147:154–162. https://doi.org/10.1016/j.jconrel.2010.05.015

Jackson L, Jones DR, Scotting P, Sottile V (2007) Adult mesenchymal stem cells: differentiation potential and therapeutic applications. J Postgrad Med 53:121–127

Johnson KE, Wilgus TA (2014) Vascular endothelial growth factor and angiogenesis in the regulation of cutaneous wound repair. Adv Wound Care 3:647–661. https://doi.org/10.1089/wound.2013.0517

Keeney M, Deveza L, Yang F (2013) Programming stem cells for therapeutic angiogenesis using biodegradable polymeric nanoparticles. J vis Exp JoVE. https://doi.org/10.3791/50736

Laiva AL, O'Brien FJ, Keogh MB (2018) Innovations in gene and growth factor delivery systems for diabetic wound healing. J Tissue Eng Regen Med 12:e296–e312. https://doi.org/10.1002/term.2443

Luli S, Di Paolo D, Perri P et al (2016) A new fluorescence-based optical imaging method to non-invasively monitor hepatic myofibroblasts in vivo. J Hepatol 65:75–83. https://doi.org/10.1016/j.jhep.2016.03.021

Maacha S, Sidahmed H, Jacob S et al (2020) Paracrine mechanisms of mesenchymal stromal cells in angiogenesis. Stem Cells Int. https://doi.org/10.1155/2020/4356359

Mitchell R, Mellows B, Sheard J et al (2019) Secretome of adipose-derived mesenchymal stem cells promotes skeletal muscle regeneration through synergistic action of extracellular vesicle cargo and soluble proteins. Stem Cell Res Ther. https://doi.org/10.1186/s13287-019-1213-1

Park KM, Gerecht S (2014) Harnessing developmental processes for vascular engineering and regeneration. Dev Camb Engl 141:2760–2769. https://doi.org/10.1242/dev.102194

Pelizzo G, Avanzini MA, Icaro Cornaglia A et al (2015) Mesenchymal stromal cells for cutaneous wound healing in a rabbit model: preclinical study applicable in the pediatric surgical setting. J Transl Med 13:219. https://doi.org/10.1186/s12967-015-0580-3

Ranganath SH, Levy O, Inamdar MS, Karp JM (2012) Harnessing the mesenchymal stem cell secretome for the treatment of cardiovascular disease. Cell Stem Cell 10:244–258. https://doi.org/10.1016/j.stem.2012.02.005

Ruifrok AC, Johnston DA (2001) Quantification of histochemical staining by color deconvolution. Anal Quant Cytol Histol 23:291–299

Salgado MI, Petroianu A, Alberti LR et al (2013) Conducted healing to treat large skin wounds. Chir Buchar Rom 108:706–710

Tremolada C, Colombo V, Ventura C (2016) Adipose tissue and mesenchymal stem cells: state of the art and Lipogems® technology development. Curr Stem Cell Rep 2:304–312. https://doi.org/10.1007/s40778-016-0053-5

Wong VW, Sorkin M, Glotzbach JP et al (2011) Surgical approaches to create murine models of human wound healing. J Biomed Biotechnol 2011:969618. https://doi.org/10.1155/2011/969618

Ziadloo A, Burks SR, Gold EM et al (2012) Enhanced homing permeability and retention of bone marrow stromal cells by noninvasive pulsed focused ultrasound. Stem Cells 30:1216–1227. https://doi.org/10.1002/stem.1099